Commissioning a passive-scattering proton therapy nozzle for accurate SOBP delivery

M. Engelsman,[a] H.-M. Lu, D. Herrup, M. Bussiere, and H. M. Kooy
Department of Radiation Oncology, Francis H. Burr Proton Therapy Center, Massachusetts General Hospital, Boston, Massachusetts 02114 and Harvard Medical School, Boston, Massachusetts 02114

Proton radiotherapy centers that currently use passively scattered proton beams do field specific calibrations for a non-negligible fraction of treatment fields, which is time and resource consuming. Our improved understanding of the passive scattering mode of the IBA universal nozzle, especially of the current modulation function, allowed us to re-commission our treatment control system for accurate delivery of SOBPs of any range and modulation, and to predict the output for each of these fields. We moved away from individual field calibrations to a state where continued quality assurance of SOBP field delivery is ensured by limited system-wide measurements that only require one hour per week. This manuscript reports on a protocol for generation of desired SOBPs and prediction of dose output. © *2009 American Association of Physicists in Medicine*.
[DOI: 10.1118/1.3121489]

I. INTRODUCTION

Proton therapy is a radiotherapy treatment modality that allows high conformality of the dose distribution to the target volume. More than 40 000 patients have been treated worldwide with proton therapy and the number of new institutes is growing rapidly. The vast majority of proton radiotherapy patients have been treated with passively scattered proton beams and this will likely remain the dominant treatment modality for the next few years. This paper relates to such passive-scattered spread-out Bragg peak (SOBP) proton radiotherapy.

A successful proton radiotherapy treatment depends on accurate delivery of the required range ($\mathbf{R}$), modulation width ($\mathbf{M}$) of the SOBP, as well as the absolute dose. The latter requires accurate determination of the dose delivered per monitor unit: The output ($\mathbf{\Psi}$).

Since the start of clinical operations at our institute, employing the IBA universal nozzle for delivery of passive-scattered SOBPs, we have delivered more than 13 000 unique clinical treatment fields. In the first few years of clinical operation, while ramping up the capacity, all fields were individually calibrated by means of computer-controlled 1D translation of an ionization chamber in a mini-water-tank. Delivery of the desired range and modulation sometimes necessitated a request from the treatment control system (TCS) for a range and modulation width that differed from the values specified in the treatment planning system (TPS). The modulation width as delivered by the TCS could differ by more than the ±3 mm accuracy requirement because the original manually optimized current modulation functions (see Sec. II A) resulted in relatively large undulations in the flat region of the SOBP (but within the ±2% SOBP uniformity requirement). The resulting modulation transfer function (see Sec. II E) was therefore not accurate enough. The requested TCS range had to be adjusted only very infre-

quently, the cause of which was that the then existing current modulation functions of the TCS for some range intervals resulted in a slightly more shallow distal falloff of the SOBP requiring an increase in the requested TCS range to match the location of the distal 90% of the SOBP as obtained from the TPS.

To the best of our knowledge, all proton radiotherapy centers that currently use passively scattered proton beams do field specific calibrations for a non-negligible fraction of treatment fields, which is time and resource consuming. Bortfeld and Schlegel[1] developed an analytical approximation for SOBPs at infinite SAD. Their model was modified by Kooy *et al.*[2] and fitted to our historical data to allow output prediction of 80% of our clinical treatment fields with acceptable accuracy. Extension of the output model to take into account a shift in the effective source position as a function of range[3] and shifting to output calibrations without patient-specific hardware[3,4] further increased the accuracy of the model. Fields with either a large or a very small modulation were, however, typically still individually measured because of uncertainties in the modulation and/or the output. Fields with a modulation of less than 3 cm, that were typically used for stereotactic radiosurgery treatments, furthermore required an increased accuracy in the modulation to ±1 mm.

The development of time-resolved depth dose scanning[5] allowed accurate optimization of current modulation functions (CMFs) for delivery of flat SOBP depth dose distributions and, most significantly in our current context, improved understanding and control of uncertainties in SOBP delivery.[6]

Our considerable familiarity with, and confidence in, our delivery system allowed us to recommission our techniques and procedures to specify $\mathbf{R}$, $\mathbf{M}$, and $\mathbf{\Psi}$ for any clinical field with confidence. We have now achieved a state where only
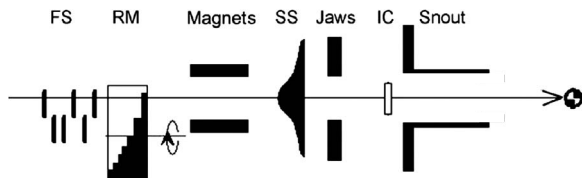
FIG. 1. Schematic, not to scale, of our IBA universal nozzle in double-scattering mode. Components are a binary fixed scatterer system (FS), a range modulator track (RM), magnets (not used for double scattering), a contoured second scatterer (SS), collimator jaws, monitor unit chamber (IC), and snout.

system-wide measurements are necessary. We report on the steps taken to achieve this model and on the accuracy of the model as determined by our routine verification measurements.

II. METHODS

II.A. Description of our nozzle

Our two proton gantries use the IBA (IBA Ltd., Louvain la Neuve, Belgium) universal nozzle. In this paper we will only discuss the commissioning of this nozzle for full control of SOBP proton radiotherapy in double-scattering mode. A schematic overview of our nozzle is shown in Fig. 1. Details of our nozzle can be found from Lu *et al.*[5] and Paganetti *et al.*,[7] but a brief description follows for increased understanding of the steps and time and effort involved in commissioning.

Our nozzle delivers flat SOBPs over a distal range interval from 4.6 to 25.0 cm (in water). This range interval is divided into seven so-called options, nonoverlapping, with each option characterized by a pair of range modulator track and second scatterer. The options are labeled A1 to A7, from lowest to highest range. An additional option A8 is special in that it has a very thin second scatterer. It therefore behaves almost like single scattering and can only deliver flat lateral dose profiles for fields up to 10 cm diameter, as opposed to the 25 cm diameter for the other options. The range interval for option A8 is from 22.8 to 29.0 cm, which partly overlaps with option A7.

The fixed lead scatterers, up to 2 mm total thickness, fine-tune the flatness of the lateral dose profile. The dose profile depends on the effective scatter in the range modulator and fixed lead scatterers. The effective scatter decreases with increased range in an option, and adding an increasing amount of lead maintains the flat profile over the option energy interval.

Almost all options can deliver up to full modulation width, in which case the flat part of the SOBP extends proximally to the patient skin. The width of an SOBP for patient treatment is controlled by the "stop digit," with a full rotation of the range modulator track divided into 256 stop digits. A fraction of each range modulator track is taken up by the "stop block," a piece of brass thick enough to stop all protons. For each rotation the beam turns on with the full beam incident on the stop block and turns off when the desired stop digit, and hence the desired modulation, is reached.

The range modulator track, constructed as a series of steps of increasing thickness and of decreasing angular width, in combination with a current modulation function ensures flatness of the SOBP in the depth direction. The CMF controls the relative current intensity as a function of stop digit and ensures that the range modulator track delivers a flat SOBP plateau. Maximum flatness is only guaranteed for a single range within the option. For other ranges the width of each pristine Bragg peak in the SOBP changes slightly, leading to a small tilt in the depth dose distribution. Therefore each option is divided into three "suboptions" that differ only in their CMF. This subdivision minimizes tilt in the SOBP as a function of range within the option to well within ±1%. In total there are 24 CMF files for a gantry. Our nozzle uses snout sizes of 12, 18, and 25 cm diameters.

We will use the term "commissioning" to denote our effort toward accurate and predictable delivery of **R**, **M**, and **Ψ** of SOBPs, i.e., toward full control of SOBP delivery. We separately baselined the nozzle such that the TCS accurately delivers a single pristine Bragg peak of desired range with irradiation of the first step of the range modulator wheel only. This includes determination of the fixed scatterer thickness required as a function of range to ensure a flat lateral dose distribution.

II.B. Standardized setup for commissioning

Several factors influence the shape of the SOBP, e.g., the jaw position, the air gap (distance between downstream side of the aperture/range compensator combination and the upstream edge of the patient or phantom), the aperture size (and therefore snout size), and the position of the isocenter with respect to the SOBP region. These factors therefore influence determination of the optimal CMF. There is therefore a need for a standardized commissioning geometry, as close to clinical patient treatments as possible;

Snout/field size: 12 cm snout and a 12 cm diameter aperture; more than 70% of our patients are treated on the 12 cm diameter snout.

Air gap: 8 cm; our standard air gap in clinical practice is 2 cm, while our mean compensator thickness is 6 cm.[8] Our reference geometry uses no range compensator as advocated by Kooy *et al.*[3] and Fontenot *et al.*[4]

Range: The CMF is optimized for the middle range in each suboption.

Isocenter: 4 cm upstream of the pristine Bragg peak range; this assumes that the average modulation width is 8 cm. For very small ranges, i.e., **R** < 8 cm, the isocenter depth is roughly at half the range.

Jaw position: 18 cm; this value expresses the physical opening between both sets of jaws at their

location along the beam line. Since the jaws are located almost halfway between the virtual source and isocenter this projects to a field size in the isocentric plane of about 36 cm. 18 cm is the maximum possible jaw opening which, due to the large virtual source size of (our) double-scattering nozzle, is necessary to ensure the maximum usable flat field size in the 25 cm diameter snout. Technically the jaw opening can be smaller when using smaller snouts but this influences the shape of the SOBP as we will show later. The over-riding reason for our choice, however, is the fact that the snout is not interlocked with the jaws which would allow delivery of a 25 cm diameter aperture with too small jaw positions. Always using the maximum jaw position prevents this at the cost of an increase in neutron dose to all patients. This increase in neutron dose is, however, less than 10% as confirmed with Monte Carlo simulations and measurements with Bonner spheres.

These settings are for optimization of the 24 CMF files. For the output prediction model and for range, modulation, and output (see Sec. II F) validation, the isocenter is always positioned at the middle of the SOBP region while maintaining an 8 cm air gap between the downstream side of the 12 cm aperture in the 12 cm snout and the CRS (Computerized Radiation Scanners Inc., Vero Beach, FL) water tank. All other settings are the same.

II.C. Redefinition of modulation width

Historically, at least in our institute, the modulation width was defined as the distance, in depth, between the proximal 90% and distal 90% isodose levels (M_{90}). This assumes that the (average over the) SOBP region is normalized to 100%. We recently changed our definition of modulation to M_{98}, i.e., the distance between the proximal 98% and distal 90% isodose levels. This has several advantages.

- The proximal 98% isodose level is on the steepest part, the proximal "knee," of the dose gradient, and therefore well defined.
- The output model for any option depends on a single parameter, $r_{small} = (R-M)/M$, and on this parameter being a positive number. For target volumes that extend very close to the patient surface, with the requirement of being uniformly covered with 100% of the prescribed dose, the entrance dose may be larger than 90% and M_{90} may therefore be undefined. In clinical practice our minimum compensator thickness is 2 mm (water equivalent), and we limit M_{98} to a maximum of the range minus 1 mm. This means that all clinically desired modulation widths fall within our model requirement of $r_{small} > 0$.
- Our aim in treatment planning (single) proton fields is
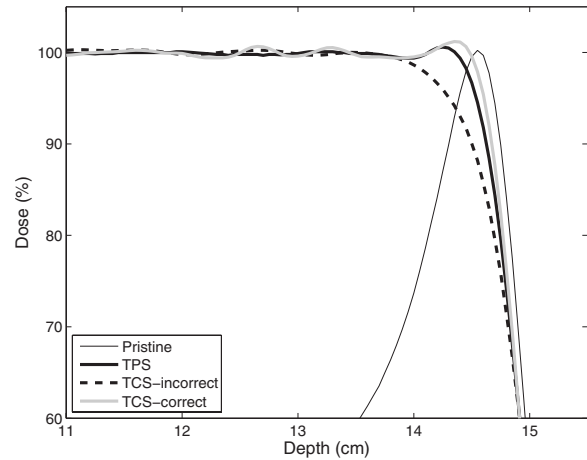
FIG. 2. Pristine Bragg peak and SOBP depth dose distributions for a range of 14.7 cm. The pristine Bragg peak was the deepest peak in all SOBPs shown. The curve labeled "TCS-incorrect" is the result of CMF optimization aimed at the flattest possible SOBP. The curve labeled "TCS-correct" is optimized toward, first, the steepest distal dose gradient and, second, a flat SOBP.

for homogeneous coverage of the tumor with 100% of the prescribed dose. M_{98} clearly is a better representation of the extent of the high dose region, and therefore of the tumor size, than M_{90}.

We maintain the use of the distal 90% isodose level in the definition of M_{98}, because our definition of range is maintained at the depth of the distal 90% isodose level of the distal pristine Bragg peak of the SOBP. Although our aim is to cover the target homogeneously with the prescribed dose, the dose gradient between the distal 98% and distal 90% isodose levels is very steep. The typical falloff distance is 2–3 mm. To spare normal tissues distal to the target, we aim for distal coverage of the target with the distal 90% (while accounting for range uncertainties). This may result in a minor underdose to only a very small volume of the target. Multiple field angles further minimize the underdosage in the target, while each field spares normal tissue distal to the target.

II.D. CMF optimization

For commissioning we use our 1D-translational CRS water tank with a Markus-type ionization chamber with the beam in the horizontal direction (gantry angle=270°). Optimization of the CMF was described by Lu and Kooy.[5] Acquisition of data for CMF optimization takes place in service mode because of the 1000 MU limit in clinical treatment mode.

As mentioned, our TCS has been commissioned to the range of pristine Bragg peaks, as has our TPS. The range of an SOBP, i.e., consisting of at least two peaks, is typically 1 mm less than the range requested from the TCS, simply because the two deepest peaks in an SOBP are stacked. This range shift can be fine-tuned by careful optimization of the CMF files. Figure 2 shows pristine Bragg peak and SOBP depth dose distributions for a (pristine Bragg peak) range of
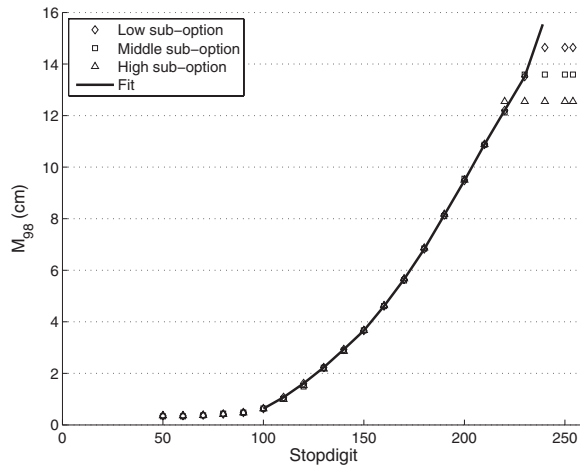
FIG. 3. Modulation as a function of stop digit for the three suboptions (high, medium, and low) of option A5. The solid line indicates the modulation transfer function as implemented in our TCS for this option.

14.7 cm. Automatic optimization aimed at the flattest possible SOBP region (the thick dashed curve) results in quite a difference compared to the SOBP as modeled by the TPS. The steepest distal dose falloff is obtained when allowing a small dip and a small peak, within the ±2% dose homogeneity constraint, in the SOBP close the distal falloff region. CMF optimization aimed at, first, a steep distal dose gradient and, second, a flat SOBP results in an SOBP that is virtually identical to the SOBP in the TPS. Now, for the same range of the deepest pristine Bragg peak, the SOBP in the TCS and in the TPS have distal ranges of 14.67 and 14.63 cm, respectively. For all SOBPs displayed in Fig. 2 the range of the deepest pristine Bragg peak, as defined by the 90% isodose level, was exactly equal.

II.E. Control of the modulation width

The data obtained from a single time-resolved depth dose scan allow optimization of the CMF as well as determination of the modulation as a function of stop digit, the "modulation transfer function." This transfer function is only defined for the option in the TCS, i.e., all three suboptions have the same transfer function. This is, however, not an issue. Figure 3 shows the modulation as a function of stop digit for option A5 (range interval of 11.65–15.54 cm). The transfer function is not defined for very small and very large stop digits. For very small stop digits, the modulation does not change because the beam always passes through the first step of the range modulator wheel only. For very large stop digits, the beam is completely stopped by the modulation wheel. For different ranges in an option this happens at different stop digits (i.e., modulation widths).

We can only measure the depth dose starting at the downstream surface of the upstream wall of the water tank, i.e., at about 8 mm water equivalent depth. This prevents us from accurately measuring M_{98} for (near-) fully modulated fields. If the maximum measured modulation, i.e., using the middle range in the highest suboption, is reached for a stop digit smaller than 255, we extrapolate our transfer function to full
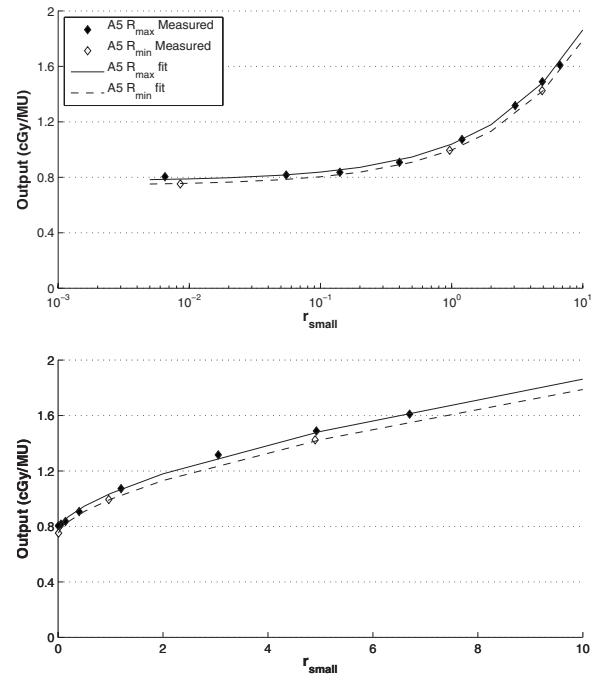
FIG. 4. Output for option A5 as a function of $\mathbf{r}_{small}$. (Top) Logarithmic scale. (Bottom) Linear scale. The output is measured at the maximum range in the option (solid) and at the minimum range (open).

modulation, i.e., maximum range in the option minus 1 mm (see Fig. 3). The error in dose in the proximal region for such a large modulation is very small as the entrance dose for an SOBP with the proximal 98% at a depth of 8 mm is around 95%, even for our smallest deliverable range of 4.6 cm.

II.F. The output model

The output model used is the one described by Kooy *et al.*[3] This model is based on the theoretical approach of Bortfeld and Schlegel[1] and includes a linear correction for the
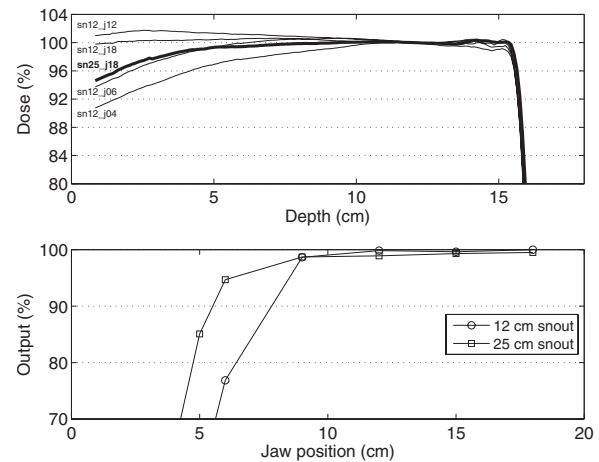
FIG. 5. Effect of jaw position on the SOBP for both the 12 and 25 cm snouts using maximum sized apertures. The SOBP had a range of 15.7 cm and full modulation. (Top) Depth dose curves, normalized at 12 cm depth with, e.g., "sn12_j18" denoting use of the 12 cm diameter snout and jaws opened to 18 cm. (Bottom) Output as a function of jaw position, as measured at a depth of 12 cm.

source shift within an option that leads to a change in output as a function of **R** for equal values of $\mathbf{r_{small}}$. The complete formula is given below:

$$\Psi(\mathbf{R},\mathbf{M}) = \left(\frac{D_{0,c} \cdot \Psi_c \cdot \mathrm{CF}}{100}\right) \cdot (1 + a_1$$
$$\cdot r_{small}^{a_2}) \cdot (a_3 + a_4 \cdot (R - R_{min})), \quad (1)$$

with

$$r_{small} = \left(\frac{\mathbf{R} - \mathbf{M_{98}}}{\mathbf{M_{98}}}\right), \quad (2)$$

where Ψ_c and $D_{0,c}$ are the output factor and SOBP entrance dose, respectively, of the reference calibration field (**R** =16 cm, $\mathbf{M_{98}}$=10 cm). Parameters CF, a_1, a_2, a_3, and a_4 are option specific parameters, with the latter two parameters describing the linear correction in the output as a function of range within the option. Parameter R_{min} is the minimum range within the option. The range correction factor is unity for the maximum range in an option.

For each option we measured the range, modulation, and output for seven to nine combinations of **R** and $\mathbf{M_{98}}$ at the maximum range in the option and for three combinations at the minimum range in the option. These measurements served to fit the output model on a per option basis and were

performed in clinical treatment mode. At the same time these measurements were used as verification of our exact control of range and modulation. As mentioned in Sec. II B, for each of these verification measurements the isocenter was located at the middle of the SOBP region and the air gap was 8 cm.

For the largest range in the option we chose the values of $\mathbf{r_{small}}$ to be more or less equidistant on a logarithmic scale, see Fig. 4(a). This results in more points in the region where the output varies faster as a function of $\mathbf{r_{small}}$, see Fig. 4(b). For the smallest range in the option we measured at the maximum modulation in the option, at the minimum modulation (which we set to 2 cm), and near $\mathbf{M_{98}}$=0.5**R**, i.e., $\mathbf{r_{small}}$=1.

III. RESULTS

III.A. Effect of jaw position

Figure 5(a) shows the depth dose distribution for a range of 15.7 cm and full modulation. The CMF was optimized for the 12 cm snout and an 18 cm jaw position. When the jaw position decreases, the proximal dose distribution first increases and then decreases. We do not have an explanation for this behavior although the complex scatter of protons inside the nozzle devices certainly is responsible. Also plotted (thick black line) is the depth dose distribution for the 25
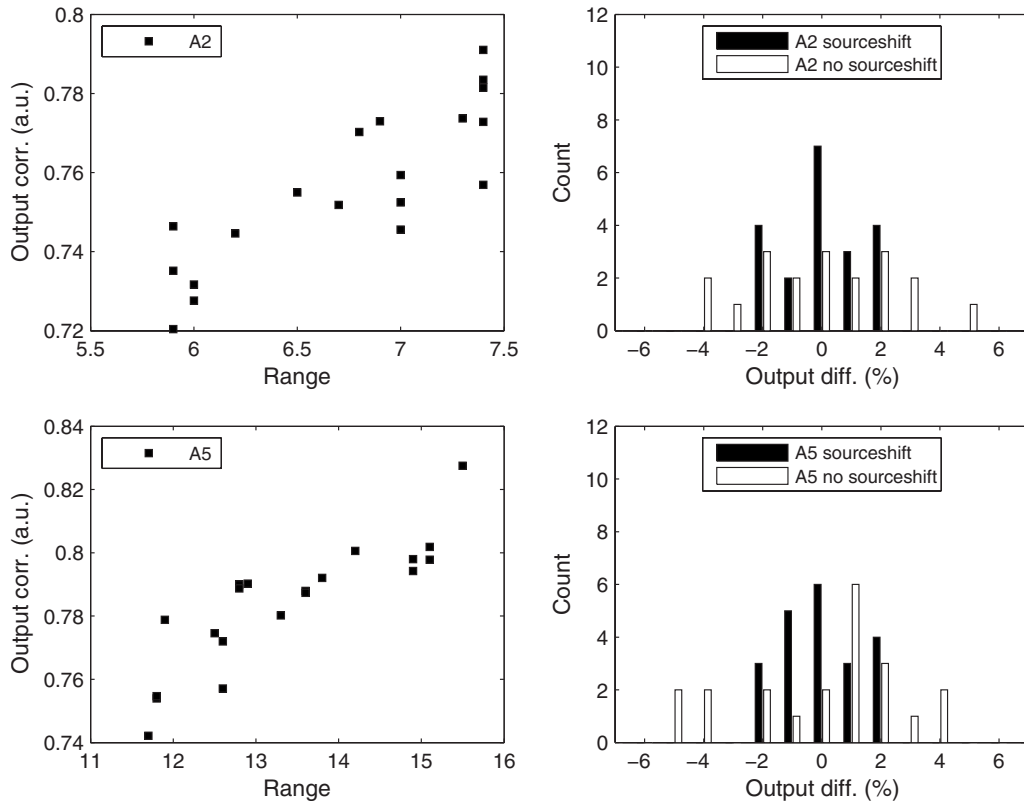
FIG. 6. Effect of the range within the option on the output for (top row) option A2 (range interval: 5.82–7.49 cm) and (bottom row) option A5 (range interval: 11.65–15.54 cm). Left hand graphs: Output as a function of range. Data are corrected for the first two terms in Eq. (1). Right hand graphs: The black columns show the accuracy of the output model, as given in Eq. (1), for historical verification data acquired since recommissioning the gantry. The white bars are for a best fit to the data when forcing the range correction term in Eq. (1) to unity.

TABLE I. Range correction factor [parameter a_4 in Eq. (1)] as a function of option. The range correction factor expresses a percentage correction in the output per cm of range change within the option. Each option spans an interval of ranges.

Option	a_4
A1	0.042
A2	0.037
A3	0.029
A4	0.024
A5	0.018
A6	0.015
A7	0.007
A8	0.002

FIG. 7. Output for all options as a function of $\mathbf{r_{small}}$. (a) Output for $\mathbf{r_{small}} \leq 1$; (b) output for $\mathbf{r_{small}} \geq 1$.

cm snout at the same clinically used 18 cm jaw position. Clearly the shape of the SOBP, and therefore the correct CMF, depends on the reference geometry used. The reduction in the proximal dose for the 25 cm snout can be explained by less in scatter of protons from the inside of the aperture (or snout) toward the central axis. The reduction in proximal dose due to this effect is not currently modeled in our treatment planning system. Use of multiple field directions mitigates the effect.

As mentioned in Sec. II B reducing the jaw position decreases the neutron dose to the patient. A jaw position of about 12 cm still ensures an appropriate flat field size for the 12 cm snout. Figure 5(b) shows the output as a function of snout size and jaw position. The effect is small over the range of jaw positions from 12 to 18 cm, that can be clinically applied for the different snouts. For the currently clinically fixed jaw position of 18 cm, the reduction in output is less than 0.5% when using the maximum field size on the large snout instead of the reference geometry of the 12 cm field size and the 12 cm snout.

III.B. Range correction in the output model

In our nozzle, the first scattering elements are the fixed scatterer system and the range modulator wheel. Each step of a range modulator track consists of two materials such that the required pullback is achieved at constant scattering "power." Rotation of the range modulator wheel thus has no influence on the virtual source position. As the range in an option increases, more fixed scatterer material is needed to maintain field flatness in the lateral direction. This is done by means of the fixed scatterer system and results in a pullback of the virtual source position. Since the isocenter and the monitor unit chamber are at fixed locations, a pullback in virtual source position, by means of the inverse-square law, results in an increase in output. The left panels in Fig. 6 show the increase in output as a function of range in the option. We have chosen to model this by means of a linear correction component in the output model, see Eq. (1). The right panels in Fig. 6 show the increased accuracy of output prediction when taking into account this linear range correction term.

As mentioned in Sec. II A, each option is characterized by a different combination of range modulator track and second
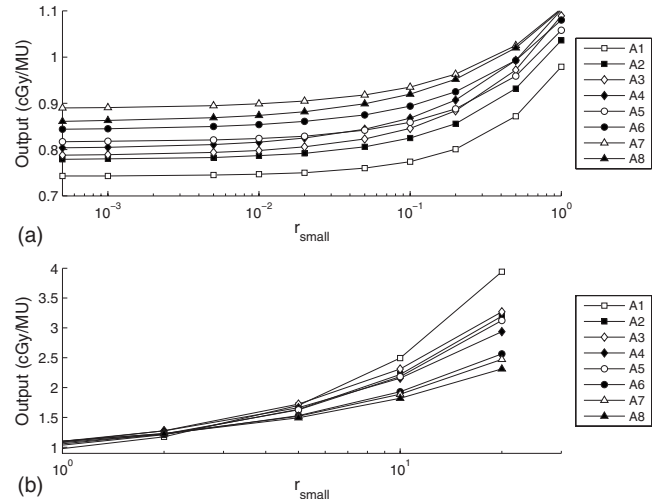
scatterer. This difference in hardware leads to substantial differences in the magnitude of the range correction parameter per cm of range within an option (second column in Table I).

III.C. Output model for different options

Figure 7 shows the output model for the highest range in each option. The different range modulator tracks and second scatterers for each option lead to each option having unique scattering properties. This in turn results in unique behavior for the output as a function of $\mathbf{r_{small}}$. Although the general behavior of each output curve is similar, it is not possible to use a single function, based on Eq. (1), to describe all options. Observing Fig. 7(a) and ignoring option A8, one may think that a single output model would perhaps be possible simply by taking into account the range correction. The output curve for the lowest range in option A6 ($\mathbf{R} = 15.6$ cm, not shown), however, does not nearly overlap with the output curve for the highest range in option A5 ($\mathbf{R} = 15.5$ cm), and similarly for other option boundaries. More importantly, the order of most output curves is reversed for large values of $\mathbf{r_{small}}$ [see Fig. 7(b)], which means that the shapes of the curves are different and a simple "shift" as executed by the range correction factor will never suffice.

III.D. Accuracy of SOBP delivery

In December 2007 we stopped the use of individual field calibrations, except for radiosurgery fields with an $\mathbf{M_{98}}$ < 2 cm. For all other fields we predict the output and have confidence in our TCS delivering the correct range and modulation. We started a program of weekly verification measurements to ensure the accuracy of our treatment control system and our output prediction model. On a weekly basis we chose for each option a random combination of $\mathbf{R}$ and $\mathbf{M_{98}}$ and performed a full calibration under the reference conditions as described in Sec. II B. Currently we perform these tests weekly, alternating between our two gantries. Acute problems with our beam delivery system will be
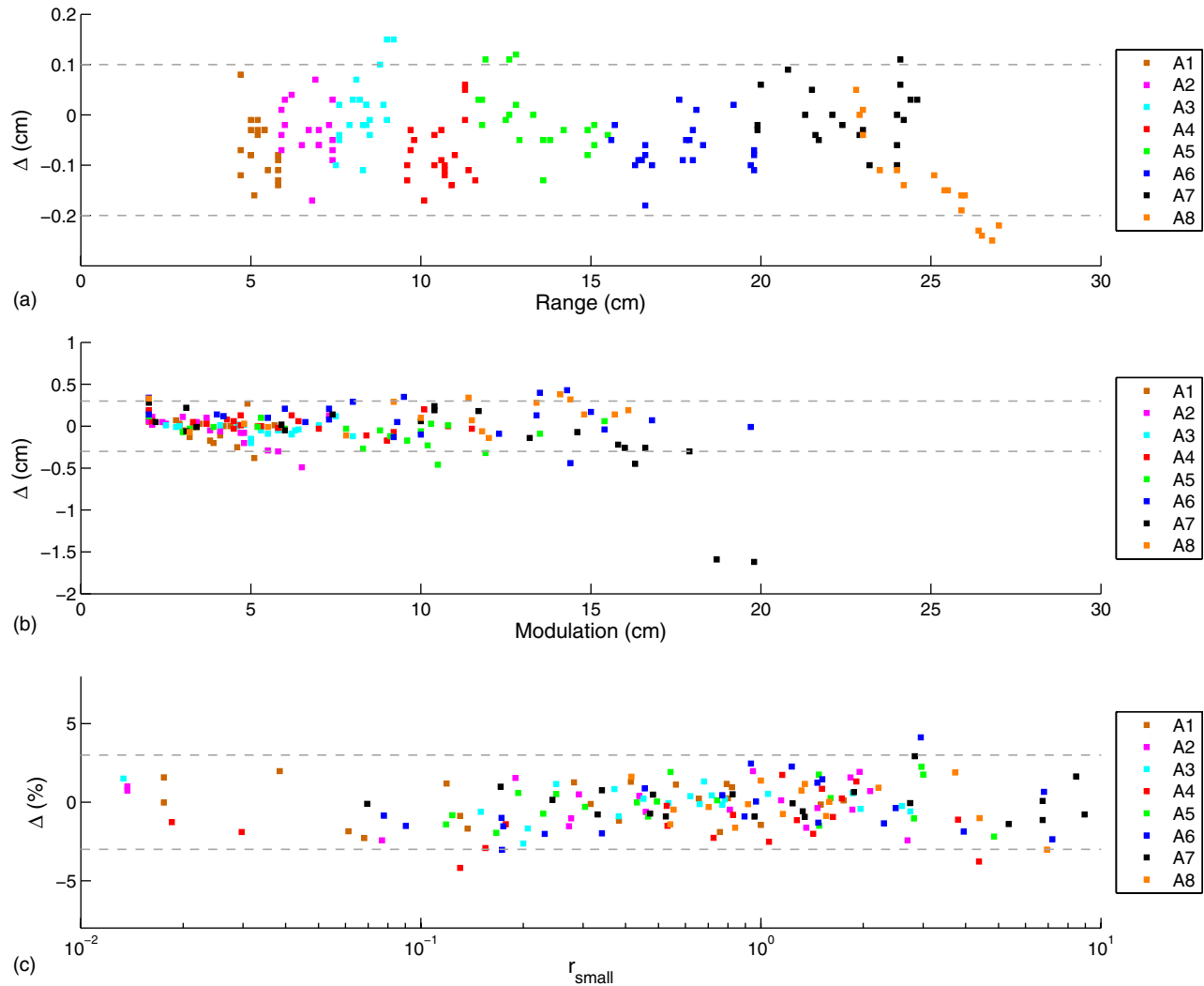
FIG. 8. Results of the weekly TCS verification. The figure shows the difference between expected and measured (a) ranges (**R**), (b) modulations (**M$_{98}$**), and (c) outputs (**Ψ**). Negative values mean that the value as measured was lower than expected. All fields for which the measured modulation differed by more than 3 mm from the requested modulation passed the 3% dose criterion, i.e., at least 95% dose at the expected location of the proximal 98% isodose level.

caught by our daily morning quality assurance procedure. Figure 8 shows the results of these weekly verification measurements and demonstrates that we have full control over our SOBPs.

III.D.1. Range

The tolerance we allow in the range is $[-1, +2]$ mm, meaning that we prefer to err on the side of extra dose to normal tissue. Since we avoid staying off critical structures by means of range, unless the structure is at least 20 mm but typically 30 mm distal of the high dose region after taking into account range uncertainty, the possible 2 mm overshoot is safe. As mentioned before, our TCS has been calibrated separately to deliver the correct range of a pristine Bragg peak. The range of an SOBP field is typically 1 mm smaller than that of the deepest peak in the SOBP. We therefore expect the ranges as measured to be within $[-2, +1]$ mm, as indicated by the dashed horizontal lines in Fig. 8(a). We have a few points where we overshoot. We only undershoot mar-

ginally for very large ranges in option A8. Although this option has been commissioned, it has, as of yet, never been used for patient treatments.

III.D.2. Modulation

For the modulation we allow a tolerance of 3 mm or 3% regarding the location of the proximal 98% isodose level. The 3 mm tolerance level is indicated in Fig. 8(b) by the dashed horizontal lines. If the position of the proximal 98% isodose level does not fall within the 3 mm tolerance we manually sample the dose at the location where it was expected to appear and validate if the dose is at least 95%, thus satisfying the 3% tolerance criterion. This latter criterion was met by all points.

III.D.3. Output

For the output we allow a tolerance of 3%, as indicated by the dashed horizontal lines in Fig. 8(c). Only very few points are outside of this tolerance level. Typically, the use of mul-

tiple treatment fields per day to the same tumor site mitigates this effect considerably. Over all options combined, the output is predicted with a mean of −0.1% and a standard deviation of 1.4%.

IV. DISCUSSION

IV.A. Limitations of the study

We realize that our methodology is only directly applicable to the IBA universal nozzle design. We do, however, believe that our success at full control of SOBP delivery of a passive-scattering proton nozzle, thereby discarding the need for individual field calibrations, is important for the radiotherapy community. Furthermore, some of the effects we described may be applicable to other nozzle designs and can serve as a warning. Especially the SOBP shape dependency on the jaw position was an unwelcome discovery. A simple change in jaw position requires almost complete recommissioning of the nozzle, i.e., CMF optimization and to a minor extent also re-establishment of the output prediction model.

Our output model is accurate under specific conditions only, of which the absence of field specific apertures and range compensators is the most prominent. Although a standard for determining the in-patient output of a passive-scattered proton field has not yet been developed, the current consensus in the proton therapy community is to perform field calibrations without the use of a range compensator. Kooy *et al.*[3] reported on relying on the treatment planning system to calculate the effect of the range compensator and in-patient scatter, and therefore not to use field specific hardware during field calibrations. Monte Carlo data by Fontenot *et al.*[4] supports this change. They showed that measurements of the output (cGy/MU) are more accurate without field specific range compensators.

Field specific apertures influence the dose on the central axis, and thereby the output, by means of collimator scatter, see, e.g., Kimstrand *et al.*[9] and Titt *et al.*[10] We have performed extensive measurements to accurately determine the effect of the patient-specific aperture size, and its distance from isocenter, on the output. These will be published in a separate paper together with data for our other beam lines.[11]

IV.B. Timeline for commissioning

It is difficult to theoretically derive the exact shape of a range modulator track to ensure a flat SOBP for a specific range and modulation. At acceptance testing of our first proton gantry, all 24 CMF files therefore had to be manually tweaked, which required many iterative depth dose scans. Additional depth dose scans were needed to determine the modulation transfer function (modulation as a function of stop digit) for each option. The calibration of the TCS for accurate delivery of pristine Bragg peaks of any range also required a large number of depth dose scans. Determining the correct combination of fixed scatterers as a function of range within an option to deliver flat lateral dose distributions at that time required the scanning of lateral dose profiles and many iterations.

The development of time-resolved scanning[5] and a thorough understanding of our nozzle[6] means that the 24 CMF files, over eight options, can now be optimized in less than a single day while simultaneously obtaining the modulation transfer function. The development or availability of commercially available multilayer ionization chambers and 2D ionization chamber arrays shortened the time to baseline pristine Bragg peak depths and fixed scatterer thicknesses also to less than 1 day.

Our set of 10–12 validation measurements for validation of range and modulation and for commissioning the output takes 1 h per option even when using our CRS water tank which is a rather slow method of determining depth dose distributions. Both the American Association of Physicists in Medicine[12] and the International Atomic Energy Agency[13] require the use of water for absolute dosimetry.

Currently, we can recommission one of our gantries in less than 100 man hours (1 week, two people), with complete SOBP control. Commissioning of our second gantry in 2004 took about 1000 man hours over 2 months, with manual patient-specific field calibrations still a necessity, though not for every field. Commissioning of our first gantry took even longer because procedures and measurement protocols still needed to be developed, as well as a clear understanding of dependencies of the various nozzle components and parameters.

IV.C. The output model

Our output model[3] uses the model originally described by Bortfeld and Schlegel.[1] They used a hypothetical "nozzle" with an infinite SAD, delivering idealized SOBPs assuming no range straggling. They derived approximate values of parameters a_1 and a_2 [see Eq. (1)] of 0.44 and 0.60, respectively. The values of these parameters for our nozzle vary between 0.24 and 0.40 and between 0.59 and 0.87, respectively. We have successfully applied the output model, with inclusion of a range correction factor, to our other nozzles. These are a fixed horizontal eye nozzle using a large library of range modulator wheels for creating flat SOBPs of any range up to 4 cm and a fixed horizontal stereotactic nozzle that uses a dual binary absorber system to create flat SOBPs up to 19 cm range. It appears that the model by Bortfeld and Schlegel[1] is applicable to any beam line (barring a range correction term) as long as the delivered SOBP is flat and the MU chamber is at the surface of the calibration phantom. For all our beam lines there is no scattering material, except air, between the MU chamber and the calibration phantom surface along the central beam axis. If there were no shift in the source position as a function of the range within an option, a single scaling factor based on the inverse-square law would compensate for our beam lines having a noninfinite SAD.

The hardware differences between options necessitated a separate fit of the output model [Eq. (1)] for each option. Furthermore, our gantries are not mirror images of each other. Although the output for many combinations of range and modulation varies only by a few percent between gantries, separate output models were needed. Complete SOBP

control does, however, allow a very smooth clinical program since patients can be easily swapped between gantries. Especially for emergency changes, e.g., when a single gantry is unexpectedly down, complete SOBP control is a huge benefit as outputs are routinely predicted for both gantries for every new patient field, and we trust the range and modulation to be accurately delivered by both gantries.

V. CONCLUSIONS

Our complete control of SOBP field delivery is valid for all new fields and predicts the range within $[-1, +2]$ mm, the modulation within 3 mm or 3% and the output within 1.4% (one SD). We currently perform weekly system-wide measurements, spot calibrations of a handful of SOBPs to validate the continuing accuracy of these predictions. Complete SOBP control has freed up extensive beam time, room time, and physicist time for other developments.

ACKNOWLEDGMENTS

[a] Electronic mail: mengelsman@partners.org

[1] T. Bortfeld and W. Schlegel, "An analytical approximation of depth-dose distributions for therapeutic proton beams," Phys. Med. Biol. **41**, 1331–1339 (1996).

[2] H. M. Kooy, M. Schaefer, S. Rosenthal, and T. Bortfeld, "Monitor unit calculations for range-modulated spread-out Bragg peak fields," Phys. Med. Biol. **48**, 2797–2808 (2003).

[3] H. M. Kooy, S. J. Rosenthal, M. Engelsman, A. Mazal, R. L. Slopsema, H. Paganetti, and J. B. Flanz, "The prediction of output factors for spread-out proton Bragg peak fields in clinical practice," Phys. Med. Biol. **50**, 5847–5856 (2005).

[4] J. D. Fontenot, W. D. Newhauser, C. Bloch, R. A. White, U. Titt, and G. Starkschall, "Determination of output factors for small proton therapy fields," Med. Phys. **34**, 489–498 (2007).

[5] H. M. Lu and H. Kooy, "Optimization of current modulation function for proton spread-out Bragg peak fields," Med. Phys. **33**, 1281–1287 (2006).

[6] H. M. Lu, R. Brett, M. Engelsman, R. Slopsema, H. Kooy, and J. Flanz, "Sensitivities in the production of spread-out Bragg peak dose distributions by passive scattering with beam current modulation," Med. Phys. **34**, 3844–3853 (2007).

[7] H. Paganetti, H. Jiang, S. Y. Lee, and H. M. Kooy, "Accurate Monte Carlo simulations for nozzle design, commissioning and quality assurance for a proton radiation therapy facility," Med. Phys. **31**, 2107–2118 (2004).

[8] S. Safai, T. Bortfeld, and M. Engelsman, "Comparison between the lateral penumbra of a collimated double-scattered beam and uncollimated scanning beam in proton radiotherapy," Phys. Med. Biol. **53**, 1729–1750 (2008).

[9] P. Kimstrand, E. Traneus, A. Ahnesjö, and N. Tilly, "Parametrization and application of scatter kernels for modeling scanned proton beam collimator scatter dose," Phys. Med. Biol. **53**, 3405–3429 (2008).

[10] U. Titt, Y. Zheng, O. N. Vassiliev, and W. D. Newhauser, "Monte Carlo investigation of collimator scatter of proton-therapy beams produced using the passive scattering method," Phys. Med. Biol. **53**, 487–504 (2008).

[11] J. Daartz, M. Engelsman, and M. R. Bussière, "Field size dependence of the output factor in passively scattered proton therapy: Influence of range, modulation, airgap and machine settings" (submitted).

[12] P. R. Almond, P. J. Biggs, B. M. Coursey, W. F. Hanson, M. S. Huq, R. Nath, and D. W. Rogers, "AAPM's TG-51 protocol for clinical reference dosimetry of high-energy photon and electron beams," Med. Phys. **26**, 1847–1870 (1999).

[13] P. Andreo, D. T. Burns, K. Hohlfeld, M. S. Huq, T. Kanai, F. Laitano, V. G. Smyth, and S. Vynckier, "Absorbed dose determination in external beam radiotherapy: An international code of practice for dosimetry based on absorbed dose to water," Technical Report Series No. 398, International Atomic Energy Agency, 2000.